Journal of the European Ceramic Society 18 (1998) 1389–1395

PII: S0955-2219(97)00136-2
0955-2219/98/$—see front matter

Preparation of Nd-doped $BaCeO_3$ Proton-conducting Ceramic and its Electrical Properties in Different Atmospheres

F. L. Chen,[a] O. Toft Sørensen,[b] G. Y. Meng[a] and D. K. Peng[a]

[a]Department of Materials Science and Engineering, University of Science and Technology of China, Hefei, Anhui 230026, People's Republic of China

[b]Materials Research Department, Risø National Laboratory DK-4000 Roskilde, Denmark

(Received 6 January 1997; revised version received 19 June 1997; accepted 3 July 1997)

Abstract

Nd-doped $BaCeO_3$ was prepared by a conventional ceramic processing technique using a special procedure to reduce calcining and sintering temperatures and to avoid possible contamination. $BaCe_{0.9}Nd_{0.1}O_{3-\alpha}$ single perovskite phase was formed when the mixture powders was calcined at $T \geq 1000°C$. Ball-milling of the calcined powders could well disperse agglomerates. Sintered at $T \geq 1300°C$, specimens with density ≥93% of the theoretical and without open porosity could be obtained. Electrical conductivity was measured in different dry atmospheres of Ar, air and O_2 and in moist air. The results showed that in dry Ar, air and O_2, the conductivity values at a given temperature were similar, and the activation energies almost identical, possibly because Nd-doped $BaCeO_3$ demonstrated predominately oxygen ion conduction in these environments. In moist air, proton conduction might predominate, leading to an increase in conductivity and a decrease in activation energy.

1 Introduction

$BaCeO_3$-based ceramics have received considerable attention in the past 15 years since they exhibit a high ionic conductivity in the family of ABO_3 perovskite-type oxides and have potential applications as the electrolytes in many novel electrochemical devices such as solid oxide fuel cells and hydrogen or steam sensors. Nd_2O_3 has been found to be an effective dopant.[1–3] Nd-doped $BaCeO_3$ ceramics acquire an ionic conductivity which exceeds that of the fluorite oxygen-ion conductor Y-doped zirconia at 600–800°C. This lower temperature range is attractive for solid oxide fuel cells and water vapour electrolyzers because of the anticipated lower costs of materials for interconnect, gas tubing and heat exchangers.[4]

Nd-doped $BaCeO_3$ are usually prepared by a conventional ceramic process consisting of calcining mixtures of the respective oxides and carbonates at elevated temperatures (≥1000°C), followed by sintering powder compacts at 1400 to 1600°C.[2,5,6] The samples holders used are usually alumina or zirconia materials. At high temperatures, there is some reaction between the sample and the sample holder, and this will undoubtedly contaminate the product and affect its electrical properties.[7,8] Accordingly, it is important to find a practical route to obtain contamination-free sintered specimens with the desired composition for use in the electrochemical devices.

The conductivity of Nd-doped $BaCeO_3$ was previously measured as a function of temperature, doping level and oxygen partial pressure (1–10^{-14} atm), and it was found to have both oxygen ionic and p-type electronic conduction.[9] Later on, the electrical property of this material was investigated in dry hydrogen and water vapour containing atmospheres, and it was then classified as a protonic conductor.[2,10] Further study revealed a transition in ionic conductivity from proton to oxygen ion conduction in H_2/O_2 fuel-cell conditions, as the temperature was increased from 600 to 1000°C.[11,12] However, for the analogous perovskites Gd-doped $BaCeO_3$ and Yb-doped $SrCeO_3$, ionic and p-/n-type electronic mixed conduction was reported, depending on the partical oxygen pressure in the working atmospheres.[13,14] The above seemingly conflicting results suggest

that the electrical properties of this material are closely related to its working atmosphere and should be investigated systematically.

In the present work, the Nd-doped $BaCeO_3$ ceramic was prepared by the conventional ceramic route with special procedures to reduce the calcining and sintering temperatures and avoid possible contamination. The electrical properties of the sintered specimens were examined by using ac impedance spectroscopy technique in different dry atmospheres of argon, air and oxygen, and in wet air.

2 Experimental

2.1 Preparation of $BaCe_{0.9}Nd_{0.1}O_{3-\alpha}$ sintered specimens

The starting materials were $BaCO_3$ (Alfa), CeO_2 (Alfa) and Nd_2O_3 (Alfa). The chemicals, mixed in a stoichiometric ratio to yield the composition $BaCe_{0.9}Nd_{0.1}O_{3-\alpha}$, were ball-milled (zirconia ball in plastic bottle) in ethanol for 36 h. The resulting slurry was then dried naturally. The dried powders were heated from 600 to 1200°C for 10 h and then examined by X-ray powder diffraction analysis (XRD, Philips, PW1078) using CuK_α radiation. Simultaneous thermogravimetric analysis (TGA) and differential thermal analysis (DTA) were carried out at a heating rate of 2°C min^{-1} in air, using a thermal analyser (NETZSCH STA 429). After calcining at 1000°C for 10 h, the powders were ground with an agate mortar, and then ball-milled in ethanol for 4 h to disperse agglomerates. The calcined product was examined by a laser-scattering particle-size distribution analyser (Malvern MasterSizer/E) and scanning electron microscopy (SEM, JEOL JSM-840). Compacts were obtained by pressing the ball-milled calcined powders, without adding binders, at 100 Mpa. The green density was 55 to 60% of theoretical density (6.35 g cm^{-3}). Subsequent sintering of pellets was carried out on a zirconia plate in air at 1200–1400°C for 10 h and at 1500°C for 2 h, with the following procedure to avoid the possible reaction between the sample and the zirconia plate: a thick layer of the calcined powders with the same composition was placed between pellet and zirconia plate. Bulk density and open porosity were measured by the Archimedes method using water as the liquid media. The 1400 and 1500°C sintered specimens were polished on SiC paper and then thermally etched at 1300°C for 2 h. The microstructure of these samples was examined by SEM.

2.2 Electrical measurements

Sintered pellets (12 mm in diameter, 1.5 mm in thickness) were polished using SiC paper and then cleaned with ethanol in an ultrasonic cleaner. Pt electrodes were applied by painting the planar faces of the ceramic pellets with platinum paste and then baking at 1000°C. The ac impedance spectroscopy was measured in the frequency range of 12–10^5 Hz using a GenRad 1689 precision RLC digibridge programmed via an IBM-compatible computer for data collection and analysis by employing the EQUIVCRT software.[15] The set-up for the conductivity measurement is illustrated in Fig. 1. The whole assembly was mounted horizontally in an electric-tube furnace with controlled gas flow (rate is 50 ml/min). 'Dry' gas was produced by first passing it through anhydrous $CaCl_2$, then an activated molecular sieve column, and finally through P_2O_5; 'wet' gas was obtained by passing through a water bubbler at 25 and 50°C, which is equivalent to a water vapour pressure of 22·76 and 92·51 Torr, respectively.

3 Results and discussion

3.1 Reaction process

The powder derived from mixing $BaCO_3$, CeO_2 and Nd_2O_3 was heated between 600 and 1200°C, at 100°C intervals, for 10 h, and the products were

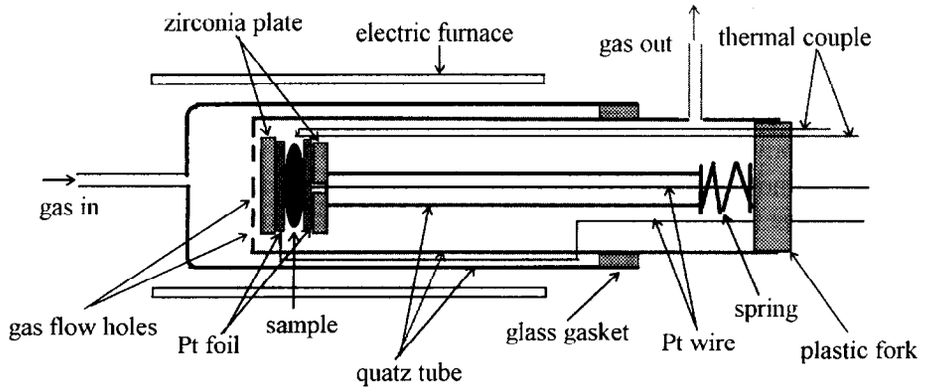

Fig. 1. The set-up for the conductivity measurement.

identified with XRD. Only starting materials were present at $T \leq 700°C$, as illustrated in Fig. 2. When the temperature was raised to 800°C, the solid state reaction was initiated, and diffraction peaks belonging to $BaCe_{0.9}Nd_{0.1}O_{3-\alpha}$ appeared. As the firing temperature was raised more $BaCe_{0.9}Nd_{0.1}O_{3-\alpha}$ was formed in the products, with a corresponding decrease in $BaCO_3$ and CeO_2. The formation of $BaCe_{0.9}Nd_{0.1}O_{3-\alpha}$ was completed when the temperature reached 1000°C, and no $BaCO_3$ and CeO_2 phases could be detected.

Simultaneous DTA–TGA was used in analysing the decomposition of $BaCO_3$ and the formation of $BaCe_{0.9}Nd_{0.1}O_{3-\alpha}$. The results are shown in Fig. 3. A small amount of weight loss occurred in the low temperature range. No difference between the as-mixed and the 600°C heated specimens could be detected by XRD examination. Accordingly, the weight loss in the low temperature range was likely to be due to the release of the absorbed water or other organic additives from the surfaces of the powders. A large weight loss began at 830°C, which is caused by the thermal decomposition of $BaCO_3$. No weight change occurred above 1100°C, indicating that the decomposition of $BaCO_3$ was complete. DTA curve indicates an endothermic peak at 806°C, which is associated with $BaCO_3$ phase transition from orthorhombic to rhombehedral.[16] An endothermic peak corresponding to the decomposition of $BaCeO_3$ was found at around 830°C. As the temperature increased, the DTA base line moved to the exothermic side, implying that the formation of $BaCe_{0.9}Nd_{0.1}O_{3-\alpha}$ is an exothermic reaction.

No intermediate compounds from the $BaCO_3$·0·9CeO_2·0·05Nd_2O_3 mixture were detected by XRD. The reaction mechanism is thus quite simple and can be expressed as:

$$BaCO_3 + 0{\cdot}9CeO_2 + 0{\cdot}05Nd_2O_3 \rightarrow BaCe_{0.9}Nd_{0.1}O_{3-\alpha} + CO_2 \quad (1)$$

XRD results reveal that the decomposition of $BaCO_3$ and the formation of $BaCe_{0.9}Nd_{0.1}O_{3-\alpha}$ complete at 1000°C, but the TGA curve shows that the above reactions finish at around 1100°C. This is due to the difference in the time spent at the measuring temperature, i.e. the XRD sample was maintained at the calcination temperature for 10 h, whereas the TGA sample was only very briefly at the corresponding temperature. Nevertheless, XRD patterns reveal that $T \geq 1000°C$ calcining of the starting materials resulted in a single perovskite-phase corresponding to that of orthorhombic $BaCeO_3$ published in JCPDS 22-74. This temperature is more than 200°C lower than that reported in the literature. Rauch *et al.*[17] reported that Gd-doped $BaCeO_3$ single perovskite phase

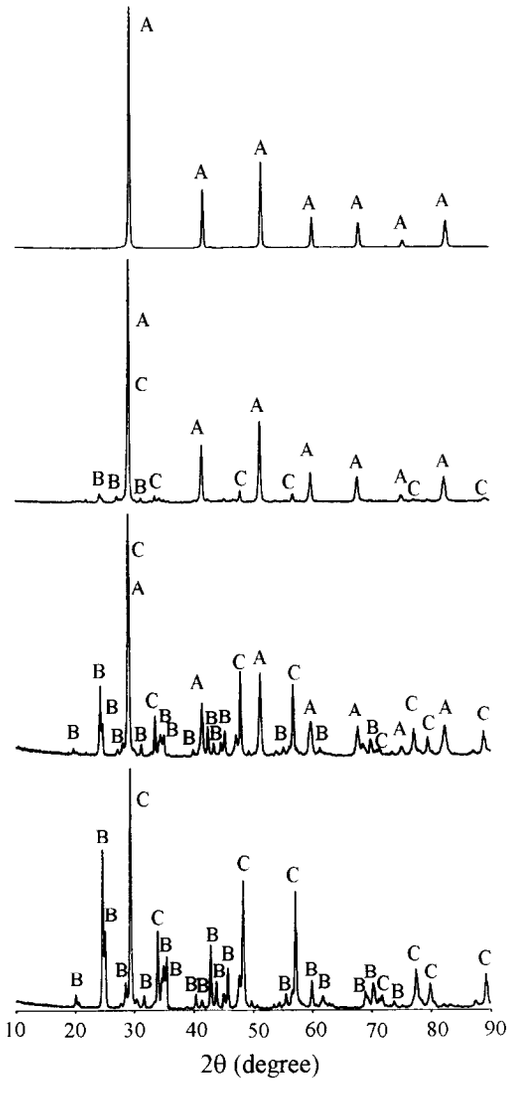

Fig. 2. X-ray diffraction patterns of the mixture of $BaCO_3$0·9$CeO_2$0·05Nd_2O_3 heated at each temperature for 10 h. A, B, and C denote diffraction peaks produced at from $BaCe_{0.9}Nd_{0.1}O_{3-\alpha}$, $BaCO_3$, and CeO_2, respectively.

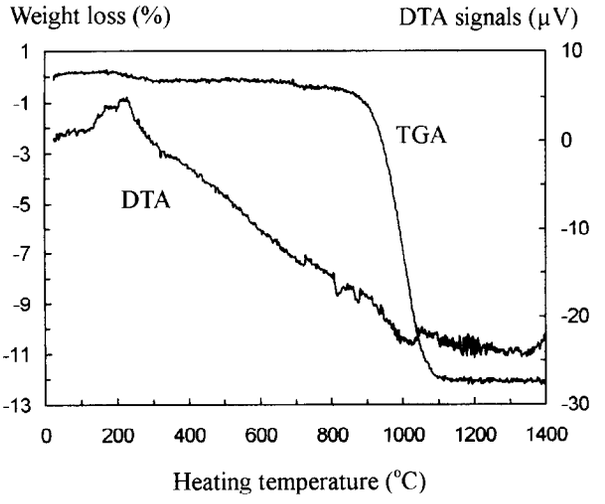

Fig. 3. Thermogravimetric analysis (TGA) and differential thermal analysis (DTA) curves of the mixture of $BaCO_3$0·9-$CeO_2$0·05Nd_2O_3.

could only be formed at about 1350°C from the solid state reaction route. Flint *et al.*[18] showed that a calcination temperature higher than 1250°C was required from a carbonate-oxide mixture to obtain $BaCe_{0.9}Gd_{0.1}O_{2.95}$ single perovskite phase. The above authors mixed their starting materials manually, while the present starting materials were mixed by ball-milling in ethanol. This process gives a more homogeneous mixtures and hence facilitates the solid state reaction. Lu *et al.*[6] also found that, by ball-milling of the starting materials, pure $BaCeO_3$ perovskite phase could be formed by calcination of $BaCO_3$ and CeO_2 mixture at 1000°C.

3.2 Characterisation of the calcined powders

Figure 4 shows the particle size distribution of the 1000°C calcined powders by different treatments. It can be noted that the mortar-ground powders consist of some agglomerates. In order to disperse the agglomerates, the calcined powders were ball-milled in ethanol. The results showed that this treatment could effectively disperse agglomerates so that small particles dominated in the ball-milled powders. As shown in Fig. 5, the calcined powders after the ball-milling treatment consist of very small, homogeneous particles with no apparent agglomerates.

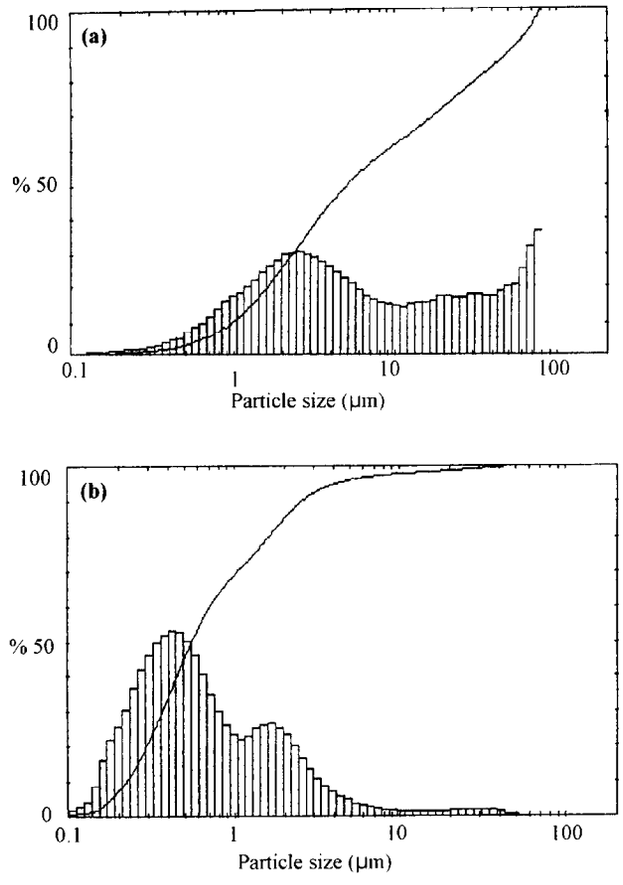

Fig. 4. Particle size distribution of the 1000°C calcined powders; (a) ground by mortar and (b) ball-milled in alcohol.

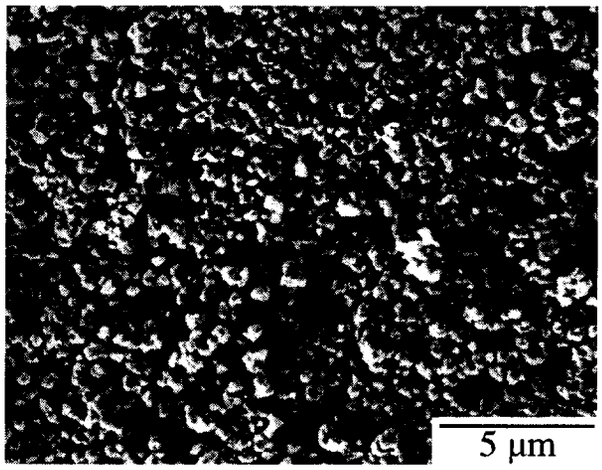

Fig. 5. Scanning electron micrographs of the ball-milled 1000°C-calcined powders.

3.3 Sintering property and microstructural evaluation

Figure 6 shows the sintered density as a function of the sintering temperature. It can be seen that when the sintering temperature exceeded 1300°C, $BaCe_{0.9}Nd_{0.1}O_{3-\alpha}$ compacts could be sintered to a density higher than 93% of the theoretical. Sintering at 1400°C for 10 h and 1500°C for 2 h resulted in a density of 97 and 99%, respectively. Open porosity results reveal that sintering at $T \geq 1300$°C, sintered specimens with no open porosity could be obtained. Figure 7 shows the surface microphotos of 1400 and 1500°C sintered specimens after polishing on SiC paper and then thermally etching at 1300°C for 2 h. Only one kind of morphology was observed with the dense microstructures. No secondary phase was detected. Working on an analogous material of Yb-doped $SrCeO_3$, Zhen *et al.*[7] reported that ball-milling (using alumina balls) introduced alumina impurity (by wear of alumina balls) which precipitated in the grain boundaries, leading to a deterioration of the electrical properties. If this were the case, the same phenomena, i.e. the segregation of zirconia in the grain boundaries caused by wear of zirconia balls, would be expected in the $BaCeO_3$ samples examined in this work. However, Fig. 7 shows no sign of such a zirconia precipitation. Therefore, the alumina impurity in the work of Zhen *et al.*[7] might come from the alumina crucible during the repeated calcination at 1673 K, since Sr^{2+} would readily react with alumina to form $SrAl_2O_4$ at temperature higher than 1200°C.[8] They found that the molar ratio of Sr/Al in the secondary phase was close to 1:2, confirming the formation of $SrAl_2O_4$. In the present work, since the calcination temperature is low (1000°C) and a special buffer (a thick layer of the calcined powders with the same composition) was used in the sintering process, so contamination from the alumina crucible was avoided.

Scholten *et al.*[16] concluded that the decomposition of organic binders added during pressing the compacts would produce carbon dioxide during sintering, and that would lead to a volume change and hence produce a low sintered density. They predicted that avoiding the use of binders and using homogeneous fine powders would produce sinters of high density. Liu *et al.*[10] found that use of the solid state reaction route to prepare Nd-doped $BaCeO_3$ without ball-milling treatment could only produce sintered samples with density about 80% of the theoretical value even when sintered at 1500°C for 12 h. The procedure employed in this work can synthesize homogeneous pre-reacted particles with small particle sizes favourable for the subsequent sintering step. Further, no organic binders were used in the present work. The high sintered density obtained in this work confirmed the predictions by Scholten *et al.*[16]

3.4 Electrical property in different atmospheres

Electrical conductivity was evaluated in the temperature range 300–700°C in different dry atmospheres of argon, air and oxygen, and in moist air. Figure 8 shows plots of $\mathrm{Ln}(\sigma T)$ versus $1/T$ in dry atmospheres. It can be noted that in the temperature range studied conductivity values are very close to one another with a slight increase in the following sequence: $\sigma(\mathrm{Ar}) < \sigma(\mathrm{air}) < \sigma(\mathrm{O_2})$. All three plots have similar slopes, indicating similar activation energy for the electrical conduction in different dry atmospheres. Figure 9 shows plots of $\mathrm{Ln}(\sigma T)$ as a function of $1/T$ in dry and moist air. It can be seen that the conductivity increased with increasing the water vapour pressure. The slopes of the conductivity plots in moist air are similar, but they are much smaller than that in dry air, indicating lower activation energy in electrical conduction in moist air.

The Arrhenius parameters can be calculated from the following expressions:

$$\sigma T = A \exp(-E_a/RT) \tag{2}$$

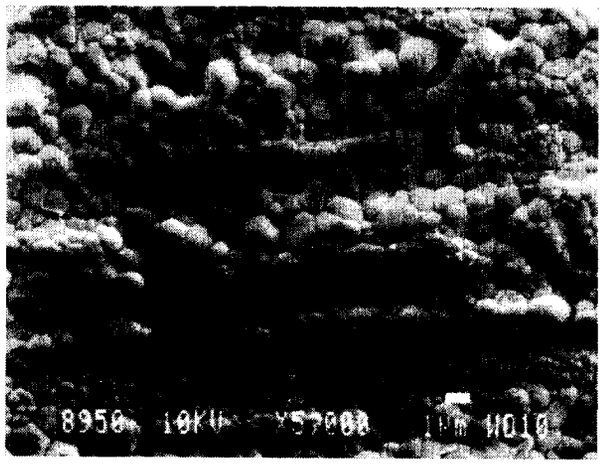

(a)

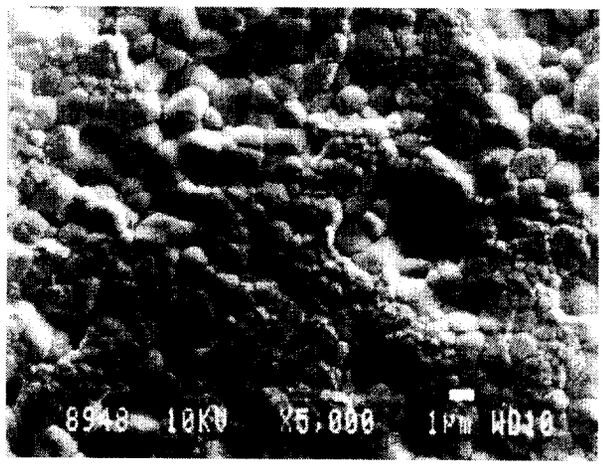

(b)

Fig. 7. Scanning electron micrographs of $BaCe_{0.9}Nd_{0.1}O_{3-\alpha}$ sintered at (a) 1400°C and (b) 1500°C.

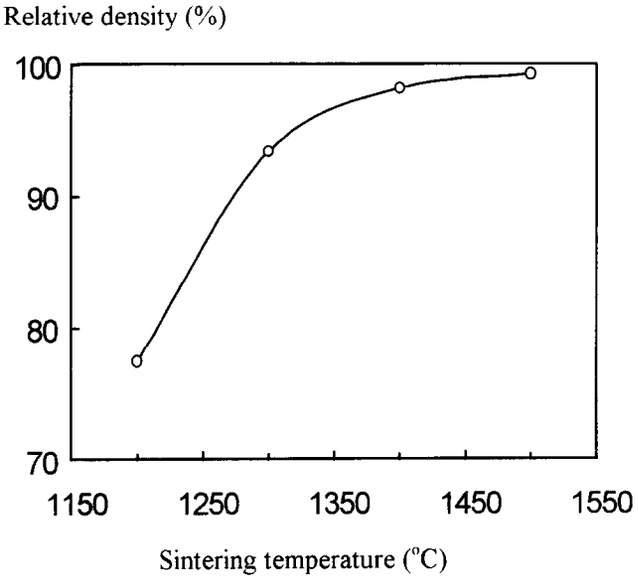

Fig. 6. Sintering density of $BaCe_{0.9}Nd_{0.1}O_{3-\alpha}$ as a function of sintering temperature.

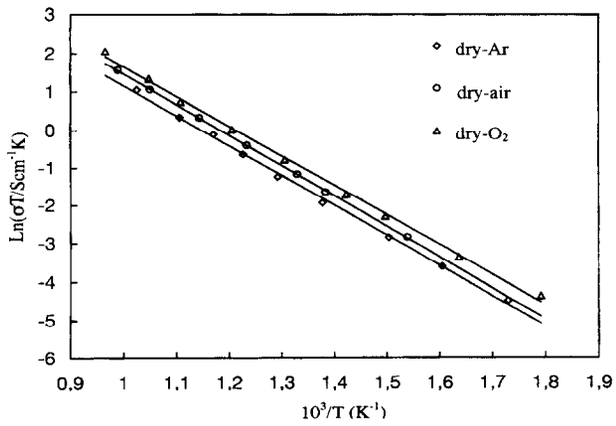

Fig. 8. Plots of $\mathrm{Ln}(\sigma T)$ versus $1/T$ in different dry atmospheres.

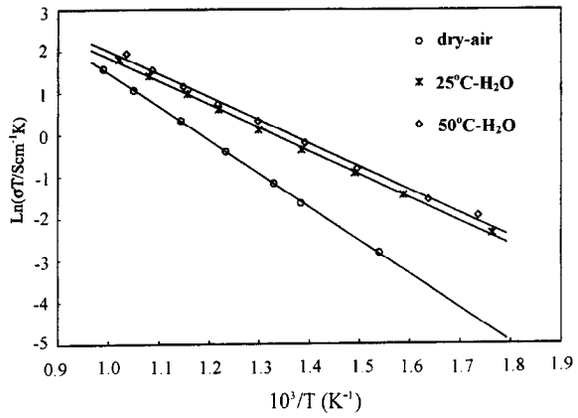

Fig. 9. Plots of Ln(σT) versus 1/T in air with different humidity.

$$\ln(\sigma T) = E_a/(RT) + \ln A \qquad (3)$$

where A is the pre-exponential factor, R is the gas constant, and E_a is the activation energy of migration. The Arrhenius parameters are listed in Table 1. The uncertainty in Ea is $\pm 0{\cdot}1\,\mathrm{kJ\,mol^{-1}}$; the uncertainty in ln$A$ is $\pm 0{\cdot}1\,\mathrm{S\,cm^{-1}\,K}$.

Table 1. The Arrhenius parameters of Nd-doped $BaCeO_3$ measured at different atmospheres.

Working atmosphere	E_a *(kJ mol^{-1})*	*InA (Scm^{-1} K)*
Ar (dry)	65.2	9.1
O_2 (dry)	64.1	9.3
Air (dry)	66.2	9.4
Air (25°C-H_2O)	46.3	7.5
Air (50°C-H_2O)	46.0	7.6

Table 1 shows that the activation energies of Nd-doped $BaCeO_3$ in dry atmospheres of Ar, air and O_2 are closely similar, and slightly smaller than values observed in the Yb-doped ceria electrolyte ($73{\cdot}2\,\mathrm{kJ\,mol^{-1}}$), which shows a very low activation energy among the fluorite oxides.[19] This indicates the relative ease with which ionic conduction occurs in the $BaCeO_3$ lattice. The activation energy of this material in moist air is much lower than that in dry air, and is only little affected by the water vapour partial pressure in the atmosphere. The pre-exponential factors is only influenced by the water vapour partial pressure in the working atmosphere, and seems not to be related to the nature of the atmosphere.

3.5 Conduction mechanism

$BaCeO_3$ in its 'pure' form is a p-type semiconductor with a limited ionic contribution to the electrical conductivity.[20] When it was doped with rare earth oxides, such as Nd_2O_3, its conductivity is greatly enhanced.[1–9] This results from the oxygen vacancies which are introduced on substitution of low valence cations Nd^{3+} on some Ce^{4+} sites. The defect reaction may be written as:

$$Nd_2O_3 \leftrightarrow 2Nd'_{ce} + V_{\ddot{o}} + 3O_o^x \qquad (4)$$

Accordingly, the oxygen vacancy is the predominant defect in Nd-doped $BaCeO_3$ ceramic. In the presence of excess oxygen, p-type conductivity in this system may come from the electron holes created by annihilation of oxygen vacancies as described by:

$$1/2O_2 + V_{\ddot{o}} \leftrightarrow O_o^x + 2\,h^{\bullet} \qquad (5)$$

In the presence of water vapour, protons are supposed to arise from high-temperature equilibrium between the condensed phase and the moist atmosphere through the following reactions:[21,22]

$$H_2O + 2\,h^{\bullet} \leftrightarrow 2H^{\bullet} + 1/2O_2 \qquad (6)$$

$$H_2O(g) + V_{\ddot{o}} + O_o^x \leftrightarrow 2OH_o^{\bullet} \qquad (7)$$

The protons then migrate according to a 'vehicular' mechanism in which the proton moves as a passenger on a larger ion such as $OH^{\bullet}$ or H_3O^+.[14]

Based on the electrical results and the above considerations, it can be concluded that, in dry atmospheres of Ar, air and O_2, Nd-doped $BaCeO_3$ demonstrates predominantly oxygen–ion conduction; the conductivities at any given temperature are similar and activation energies almost identical. The slight increase in conductivity in the sequence $\sigma(\mathrm{Ar}) < \sigma(\mathrm{air}) < \sigma(O_2)$ may be due to a slight increase in p-type electronic conduction with increasing oxygen partial pressure. In moist air, proton conduction may predominate, leading to a decrease in activation energy.

4 Conclusions

The single-phase perovskite $BaCe_{0{\cdot}9}Nd_{0{\cdot}1}O_{3-\alpha}$ was formed on $T \geq 1000°C$ calcination of the powder mixture of $BaCO_3$, CeO_2 and Nd_2O_3, obtained by ball-milling in ethanol. Ball-milling of the calcined powders in ethanol could well disperse agglomerates. Samples with no open porosity and densities higher than 93% of the theoretical could be obtained by sintering pressed compacts at $T \geq 1300°C$.

Electrical conductivities were measured in different dry atmospheres of Ar, air and O_2, and in moist air. The conductivities at any given temperature were similar and the activation energies almost identical, given Nd-doped $BaCeO_3$ exhibits predominantly oxygen–ion conduction in these

atmospheres. In moist air, proton conduction may predominate, leading to an increase in conductivity and a decrease in activation energy.

Acknowledgements

This work is supported by the National Natural Science Foundation of China. Fanglin Chen is grateful to Danish International Development Assistance (Danida) and the State Science and Technology Commission (SSTC) of China for funding this joint Ph.D study at Materials Research Department, Risø National Laboratory, Denmark. Dr N. Bonanos at Risø National Laboratory is acknowledged for his constant interest and encouragement to this work. Special thanks are given to P. Wang, T. Strauss and P. Jensen for the experimental assistance.

References

1. Iwahara, H., Esaka, T., Uchida, H. and Maeda, N., Proton conduction in sintered oxides and its application to steam electrolysis for hydrogen production. *Solid State Ionics*, 1981, **3/4**, 359–363.
2. Iwahara, H., Uchida, H., Ono, K. and Ogaki, K., Proton conduction in sintered oxides based on $BaCeO_3$. *Journal of the Electrochemical Society*, 1988, **135**, 529–533.
3. Slade, R. C. T. and Singh, N., Systematic examination of hydrogen ion conduction in rare-earth doped barium cerate ceramics. *Solid State Ionics*, 1991, **46**, 111–115.
4. Ranlov, J., Lebech, B. and Nielsen, K., Neutron diffraction investigation of the atomic defect structure of Y-doped $SrCeO_3$, a high-temperature protonic conductor. *Journal of Material Chemistry*, 1995, **5**, 743–747.
5. Stevenson, D. A., Jiang, N., Buchman, R. M. B. and Henn, F. E. G., Characterization of Ga, Yb and Nd doped barium cerates as proton conductors. *Solid State Ionics*, 1993, **62**, 279–285.
6. Lu, C. H. and DeJonghe, L. C., Influence of Nd_2O_3 doping on the reaction process and sintering behavior of $BaCeO_3$. *Journal of the American Ceramic Society*, 1994, **77**, 2523–2528.
7. Zheng, M. H. and Zhu, B., Proton conductivity in Yb-doped strontium cerates. *Solid State Ionics*, 1995, **80**, 59–65.
8. Chen, F. L., Sorensen, T. O., Meng, G. Y. and Peng, D. K., Chemical stability study of $BaCe_{0.9}Nd_{0.1}O_{3-\alpha}$ high-temperature proton-conducting ceramic. *Journal of Material Chemistry*, 1997, **7**, 481–485.
9. Paria, M. K. and Maiti, H. S., Electrical conduction in barium cerate doped with M_2O_3 (M = La, Nd, Ho). *Solid State Ionics*, 1984, **13**, 285–292.
10. Liu, J. F. and Nowick, A. S., The incorporation and migration of protons in Nd-doped $BaCeO_3$. *Solid State Ionics*, 1992, **50**, 131–138.
11. Yajima, T., Iwahara, H. and Uchida, H., Protonic and oxide ionic conduction in $BaCeO_3$-based ceramics—effect of partial substitution for Ba in $BaCe_{0.9}Nd_{0.1}O_{3-\alpha}$ with Ca. *Solid State Ionics*, 1991, **47**, 117–124.
12. Iwahara, H., Yajima, T. and Uchida, H., Effect of ionic radii of dopants on mixed ionic conduction ($H^+ + O^{2-}$) in $BaCeO_3$-based electrolytes. *Solid State Ionics*, 1994, **70/71**, 267–271.
13. Bonanos, N., Ellis, B. and Mahmood, M. N., Construction and operation of fuel cells based on the solid electrolyte $BaCeO_3$:Gd. *Solid State Ionics*, 1991, **44**, 305–311.
14. Kosacki, I. and Tuller, H. L., Mixed conductivity in $SrCe_{0.95}Yb_{0.05}O_3$ protonic conductor. *Solid State Ionics*, 1995, **80**, 223–229.
15. Boukamp, B. A., A nonlinear least squares fit procedure for analysis of immittance data of electrochemical systems. *Solid State Ionics*, 1986, **20**, 31–44.
16. Scholten, M. J., Schoonman, J., VanMiltenburg, J. C. and Oonk, H. A. J., Synthesis of strontium and barium cerate and their reaction with carbon dioxide. *Solid State Ionics*, 1993, **61**, 83–91.
17. Rauch, W. and Liu, M. L., Effect of microstructure and dopant on the electrochemical properties of barium cerate-based electrolyte. In *Ceramics Transactions*, Vol. 65, ed. P. N. Kumta, G. S. Rohrer and U. Balachandran. The American Ceramic Society, Westville, OH, 1996, pp. 73–83.
18. Flint, S. D. and Slade, R. C. T., Comparison of calcium-doped barium cerate solid electrolytes prepared by different routes. *Solid State Ionics*, 1995, **77**, 215–221.
19. Tuller, H. L. and Nowick, A. S., Doped ceria as a solid oxide electrolyte. *Journal of the Electrochemical Society*, 1975, **122**, 255–259.
20. Longo, V., Ricciardiello, F. and Sbaizero, O., Alkaline earth cerate: preparation, technical characteristics and electrical properties. In *Energy and Ceramics*, ed. P. Vincenzini. Elsevier, Amsterdam, 1980, pp. 1123–1130.
21. Uchida, H., Yoshikawa, H. and Iwahara, H., Dissolution of water vapor (or hydrogen) and proton conduction in $SrCeO_3$-based oxides at high temperature. *Solid State Ionics*, 1989, **35**, 229–234.
22. Slade, R. C. T. and Singh, N., Generation of charge carriers and an H/D isotope effect in proton-conducting barium cerate ceramics. *Journal of Material Chemistry*, 1991, **1**, 441–445.